Spatial-domain-based multidimensional modulation for multi-Tb/s serial optical transmission

Ivan B. Djordjevic,[1,*] Murat Arabaci,[1] Lei Xu,[2] and Ting Wang[2]

[1]*University of Arizona, Depart. Electrical & Computer Eng., 1230 E. Speedway Blvd., Tucson, Arizona 85721, USA*
[2]*NEC Laboratories America, 4 Independence Way, Princeton, New Jersey 08540, USA*
**ivan@ece.arizona.edu*

Abstract: The multidimensional channel capacity studies indicate that the employment of multiple photon degrees of freedom—such as subcarrier, amplitude, phase, polarization, and space—can improve the spectral efficiency by several orders of magnitude higher than that claimed in any fiber-optic experiment reported to date. This dramatic increase in spectral efficiency through multiple photon degrees of freedom can provide revolutionary capabilities for future optical networks. Moreover, photons can carry both spin angular momentum (SAM) associated with polarization, and orbital angular momentum (OAM) associated with the azimuthal phase of the complex electric field. Because OAM eigenstates are orthogonal, an arbitrary number of bits per photon can be transmitted in principle. The ability to generate the OAM modes, such as Bessel modes, in multimode fibers (MMFs) will allow realization of fiber-optic communication networks with ultra-high bits-per-photon efficiencies. To this end, we propose here a spatial-domain-based multidimensional coded-modulation scheme as an enabling technology for multi-Tb/s serial optical transport. To demonstrate the capabilities of the proposed scheme, we show that an eight-dimensional (8D) spatial-domain-based coded modulation scheme outperforms a prior-art 128-point 4D scheme by 3.88 dB at BER of 10^{-8} while providing 120 Gb/s higher aggregate information bit rate. The proposed 8D scheme also outperforms its conventional polarization-multiplexed QAM counterpart by even a larger, and indeed striking, margin of 8.39 dB (also at the BER of 10^{-8}).

OCIS codes: (060.0060) Fiber optics and optical communications; (060.4080) Modulation; (060.1660) Coherent communications; (060.4230) Multiplexing; (060.2340) Fiber optics components.

References and links

1. M. Cvijetic, *Optical Transmission Systems Engineering* (Artech House, Inc., 2004).
2. W. Shieh and I. Djordjevic, *OFDM for Optical Communications* (Elsevier/Academic Press, 2009).
3. P. Winzer, "Beyond 100G ethernet," IEEE Commun. Mag. **48**(7), 26–30 (2010).
4. J. McDonough, "Moving standards to 100 GbE and beyond," IEEE Commun. Mag. **45**(11), 6–9 (2007).
5. I. Djordjevic, H. G. Batshon, L. Xu, and T. Wang, "Four-dimensional optical multiband-OFDM for beyond 1.4 Tb/s serial optical transmission," Opt. Express **19**(2), 876–882 (2011).
6. H. G. Batshon, I. B. Djordjevic, L. Xu, and T. Wang, "Modified hybrid subcarrier/amplitude/ phase/polarization LDPC-coded modulation for 400 Gb/s optical transmission and beyond," Opt. Express **18**(13), 14108–14113 (2010).
7. H. G. Batshon, I. B. Djordjevic, and T. Schmidt, "Ultra high speed optical transmission using subcarrier-multiplexed four-dimensional LDPC-coded modulation," Opt. Express **18**(19), 20546–20551 (2010).
8. I. B. Djordjevic and M. Arabaci, "LDPC-coded orbital angular momentum (OAM) modulation for free-space optical communication," Opt. Express **18**(24), 24722–24728 (2010).
9. G. Gibson, J. Courtial, M. Padgett, M. Vasnetsov, V. Pas'ko, S. Barnett, and S. Franke-Arnold, "Free-space information transfer using light beams carrying orbital angular momentum," Opt. Express **12**(22), 5448–5456 (2004).

#142928 - $15.00 USD Received 18 Feb 2011; revised 17 Mar 2011; accepted 18 Mar 2011; published 24 Mar 2011

10. J. A. Anguita, M. A. Neifeld, and B. V. Vasic, "Turbulence-induced channel crosstalk in an orbital angular momentum-multiplexed free-space optical link," Appl. Opt. **47**(13), 2414–2429 (2008).
11. I. Gasulla and J. Capmany, "1 Tb/s x km multimode fiber link combining WDM transmission and low-linewidth lasers," Opt. Express **16**(11), 8033–8038 (2008).
12. Z. Tong, Q. Yang, Y. Ma, and W. Shieh, "21.4 Gb/s coherent optical OFDM transmission over multimode fiber," in *Opto-Electronics and Communications Conference and the Australian Conference on Optical Fibre Technology* (Engineers Australia and the Australian Optical Society, 2008), paper PDP-5.
13. S. Murshid, B. Grossman, and P. Narakorn, "Spatial domain multiplexing: a new dimension in fiber optic multiplexing," Opt. Laser Technol. **40**(8), 1030–1036 (2008).
14. S. Murshid, B. Grossman, and P. Narakorn, "Methods and apparatus for spatial domain multiplexing in optical fiber communications," US Patent No. 7,174,067 (2006).
15. S. Murshid and J. Iqbal, "Spatial combination of optical channels in a multimode waveguide," in *Frontiers in Optics*, OSA Technical Digest (CD) (Optical Society of America, 2010), paper JWA32.
16. S. Murshid and J. Iqbal, "Array of concentric CMOS photodiodes for detection and de-multiplexing of spatially modulated optical channels," Opt. Laser Technol. **41**(6), 764–769 (2009).
17. S. Murshid, A. Chakravarty, and R. Biswas, "Simultaneous transmission of two channels operating at the same wavelength in standard multimode fibers," in *Conference on Lasers and Electro-Optics/Quantum Electronics and Laser Science Conference and Photonic Applications Systems Technologies*, OSA Technical Digest (CD) (Optical Society of America, 2008), paper JWA107.
18. S. Murshid and A. Chakravarty, "Tapered optical fiber quadruples bandwidth of multimode silica fibers using same wavelength," in *Frontiers in Optics*, OSA Technical Digest (CD) (Optical Society of America, 2010), paper FWI2.
19. A. Li, A. Al Amin, X. Chen, and W. Shieh, "Reception of mode and polarization multiplexed 107-Gb/s CO-OFDM signal over a two-mode fiber," in *Optical Fiber Communication Conference/National Fiber Optic Engineers Conference (OFC/NFOEC)*, postdeadline papers (Optical Society of America, 2011), paper PDPB8.
20. M. Salsi, C. Koebele, D. Sperti, P. Tran, P. Brindel, H. Mardoyan, S. Bigo, A. Boutin, F. Verluise, P. Sillard, M. Bigot-Astruc, L. Provost, F. Cerou, and G. Charlet, "Transmission at 2x100Gb/s, over two modes of 40km-long prototype few-mode fiber, using LCOS-based mode multiplexer and demultiplexer," in *Optical Fiber Communication Conference/National Fiber Optic Engineers Conference (OFC/NFOEC)*, postdeadline papers (Optical Society of America, 2011), paper PDPB9.
21. R. Ryf, S. Randel, A. H. Gnauck, C. Bolle, R.-J. Essiambre, P. Winzer, D. W. Peckham, A. McCurdy, and R. Lingle, "Space-division multiplexing over 10 km of three-mode fiber using coherent 6 × 6 MIMO processing," in *Optical Fiber Communication Conference/National Fiber Optic Engineers Conference (OFC/NFOEC)*, postdeadline papers (Optical Society of America, 2011), paper PDPB10.
22. J. Sakaguchi, Y. Awaji, N. Wada, A. Kanno, T. Kawanishi, T. Hayashi, T. Taru, T. Kobayashi, and M. Watanabe, "109-Tb/s (7×97×172-Gb/s SDM/WDM/PDM) QPSK transmission though 16.8-km homogeneous multi-core fiber," in *Optical Fiber Communication Conference/National Fiber Optic Engineers Conference (OFC/NFOEC)*, postdeadline papers (Optical Society of America, 2011), paper PDPB6.
23. B. Zhu, T. Taunay, M. Fishteyn, X. Liu, S. Chandrasekhar, M. Yan, J. Fini, E. Monberg, F. Dimarcello, K. Abedin, P. Wisk, D. Peckham, and P. Dziedzic, "Space-, wavelength-, polarization-division multiplexed transmission of 56-Tb/s over a 76.8-km seven-core fiber," in *Optical Fiber Communication Conference/National Fiber Optic Engineers Conference (OFC/NFOEC)*, postdeadline papers (Optical Society of America, 2011), Paper PDPB7.
24. J. Sakai, K. Kitayama, M. Ikeda, Y. Kato, and K. Tatsuya, "Design considerations of broadband dual-mode optical fibers," IEEE Trans. Microw. Theory Tech. **26**(9), 658–665 (1978).
25. D. Marcuse, "Pulse propagation in two-mode waveguide," Bell Syst. Tech. J. **51**, 1785–1791 (1972).
26. M. Cvijetic, "Dual-mode optical fibers with zero intermodal dispersion," Opt. Quantum Electron. **16**(4), 307–317 (1984).
27. M. Cvijetic, *Digital Optical Communications* (Naučna Knjiga, 1989).
28. R. Nagarajan, C. H. Joyner, R. P. Schneider, J. S. Bostak, T. Butrie, A. G. Dentai, V. G. Dominic, P. W. Evans, M. Kato, M. Kauffman, D. J. H. Lambert, S. K. Mathis, A. Mathur, R. H. Miles, M. L. Mitchell, M. J. Missey, S. Murthy, A. C. Nilsson, F. H. Peters, S. C. Pennypacker, J. L. Pleumeekers, R. A. Salvatore, R. K. Schlenker, R. B. Taylor, Huan-Shang Tsai, M. F. Van Leeuwen, J. Webjorn, M. Ziari, D. Perkins, J. Singh, S. G. Grubb, M. S. Reffle, D. G. Mehuys, F. A. Kish, and D. F. Welch, "Large-scale photonic integrated circuits," IEEE J. Sel. Top. Quantum Electron. **11**(1), 50–65 (2005).
29. J. D. Jackson, *Classical Electrodynamics* (John Wiley & Sons Inc, 1975).
30. A. W. Snyder and J. D. Love, *Optical Waveguide Theory* (Chapman and Hall, London, 1983).
31. I. B. Djordjevic, M. Arabaci, and L. Minkov, "Next generation FEC for high-capacity communication in optical transport networks," J. Lightwave Technol. **27**(16), 3518–3530 (2009).
32. G. P. Agrawal, *Fiber-Optic Communication Systems* (John Wiley & Sons, 2002).
33. A. A. Savchenkov, A. B. Matsko, I. Grudinin, E. A. Savchenkova, D. Strekalov, and L. Maleki, "Optical vortices with large orbital momentum: generation and interference," Opt. Express **14**(7), 2888–2897 (2006).
34. C. Gunn, "CMOS photonics for high-speed interconnects," IEEE Micro **26**(2), 58–66 (2006).

#142928 - $15.00 USD Received 18 Feb 2011; revised 17 Mar 2011; accepted 18 Mar 2011; published 24 Mar 2011

1. Introduction

The time that we live, also known as the information era, is closely related to the Internet technology and characterized by never-ending demands for higher information capacity and distance-independent connectivity [1]. Despite the so-called "the Internet bubble" in the equity market, the Internet traffic has continued its rapid growth. Some new multimedia applications have emerged, increasing the demand for higher bandwidths. CISCO's projection of the Internet traffic growth shows an exponential dependence from 2002 to 2012 [2]. This exponential growth places an enormous pressure on the underlying information infrastructure at every level, from the core to access networks. The IP backbones have grown so quickly that some large Internet service providers have already reported router-to-router trunk connectivity exceeding 100 Gb/s in 2007 [2]. Hence, some industry experts believe that the 100 Gb/s Ethernet (100 GbE) standard adopted recently (IEEE 802.3ba) [3] came too late and that 1 Tb/s Ethernet (1 TbE) standard should be available by 2013 [4].

The multidimensional coded-modulation studies conducted in our recent publications [5–7] indicate that employment of multiple photon degrees of freedom—such as frequency, amplitude, phase, and polarization—can improve the photon efficiency by several orders of magnitude higher than that claimed in any fiber-optic experiment reported to date. This dramatic increase in photon efficiency through multiple photon degrees of freedom will provide revolutionary capabilities for future optical networks. Furthermore, it is well-known that photons can carry both spin angular momentum (SAM) and orbital angular momentum (OAM). SAM is associated with polarization, given by $\sigma\hbar$, where $\sigma = \pm 1$ for circular polarization (and where $\hbar$ is the reduced Planck constant). OAM is associated with the azimuthal phase of the complex electric field [8–10]. Each photon with azimuthal phase dependence of the form $\exp(jm\phi)$ ($m = 0, \pm 1, \pm 2, \ldots$) can carry an OAM of $m\hbar$. We can associate with each photon a total angular momentum (TAM) given by the sum of SAM and OAM, whose eigenvalues are given by $i\hbar$, where $i = \sigma + m$. Because OAM eigenstates are orthogonal, an arbitrary number of bits per photon can be transmitted in principle. We should note that until recently, the use of OAM modes for multiplexing and modulation has been studied only for free-space optical communication. Their use in optical fiber communications is yet to be unearthed. We believe that this paper is an important step toward this goal.

In [13–21], it was shown that OAM modes can be successfully excited in multimode fibers (MMFs). However, MMFs have been traditionally considered as viable mediums of transmission for only short-reach optical communication applications [11]. On the other hand, as shown by Shieh's group [12], a 21.4 Gb/s polarization-multiplexed coherent OFDM transmission over 200 km can be achieved by employing the central MMF mode only. When we compare the traditional [11] and few mode approaches [12,19–21], we see that with few mode approaches the reach and the aggregate data rate can be improved. Another approach for improving the aggregate data rate is spatial-domain multiplexing in combination with multicore fibers [22,23]. Notice that various approaches discussed in [13–23] are related to mode-multiplexing/spatial-domain-multiplexing.

As aforementioned, OAM eigenstates are orthogonal, and can be used as basis functions for multidimensional modulation schemes. Consequently, by using OAM modes, we cannot only achieve dramatic improvements in photon efficiency but also extend the reach since we reduce intermodal dispersion by exploiting the orthogonality between the OAM modes. In addition, by employing multidimensional signal constellations, compared to traditional two-dimensional signal constellations, we can increase the Euclidean distance among constellation points for the same symbol energy improving overall performance and system reach. Taking into account the following additional advantages of MMFs over SMFs, such an approach would lead to revolutionary capabilities in future optical communication networks. When compared to SMFs, MMFs offer (i) easier installation, maintenance and handling, which leads to lower-cost systems; (ii) larger effective cross-sectional area, which increases the immunity to fiber nonlinearities; and (iii) many modes for transmission, which improves the spectral

#142928 - $15.00 USD Received 18 Feb 2011; revised 17 Mar 2011; accepted 18 Mar 2011; published 24 Mar 2011

efficiency when an MMF is treated as a multiple-input multiple-output (MIMO) channel in a similar methodology used in wireless communications.

In this paper, we propose a technology that can exploit the advantages mentioned above. Specifically, in order to enable ultra-high-speed fiber-optic communication with multi-Tb/s serial data rates, we propose a multidimensional coded modulation scheme featuring $2L+1$ OAM modes $\{-L, \ldots, -3, -1, 1, 3, \ldots, L\}$. To demonstrate the capabilities of the proposed scheme, we show via Monte Carlo simulations that an eight-dimensional (8D) spatial-domain-based coded modulation scheme outperforms its corresponding prior-art 4D counterpart presented in [7] by 3.88 dB at the bit error rate (BER) of 10^{-8} while outperforming its corresponding conventional polarization-multiplexed QAM counterpart by even a larger margin of 8.39 dB (also at the BER of 10^{-8}).

The remainder of the paper is organized as follows. In Section 2, we briefly discuss the principles of spatial-domain modulation and multiplexing. In Section 3, we describe the proposed MMF based optical network for multi-Tb/s serial optical transport, identify its key optical components, and describe how these components can be implemented. The proposed spatial-domain-based low-density parity-check (LDPC)-coded modulation scheme is then described in Section 4. We present our numerical results and discuss their significance in Section 5. Finally, some important concluding remarks are given in Section 6.

2. Principles of spatial-domain modulation and multiplexing

As we mentioned in the Introduction, photons can carry both SAM and OAM. SAM is associated with polarization while OAM is associated with the azimuthal phase of the complex electric field. The angular momentum, **L**, of the classical electromagnetic field can be written as [29]

$$\mathbf{L} = \frac{1}{4\pi c}\int_V \mathbf{E}\times\mathbf{A}\, dV + \frac{1}{4\pi c}\int_V \sum\nolimits_{k=x,y,z} E_k \left(\mathbf{r}\times\nabla\right) A_k \, dV, \tag{1}$$

where **E** is the electric field intensity, **A** is the vector potential, and c is the speed of light. **A** is related to the magnetic field intensity **H** by $\mathbf{H} = \nabla\times\mathbf{A}$, and to the electric field intensity **E** by $\mathbf{E} = c^{-1}\partial\mathbf{A}/\partial t$. The second term in Eq. (1) is identified as the OAM due to the presence of the angular momentum operator $\mathbf{r}\times\nabla$. Among various optical beams that can carry OAM, Laguerre-Gaussian (LG), vortex and Bessel beams stand out since they can be easily implemented. For example, the field distribution of an LG beam traveling along the z-axis can be expressed in cylindrical coordinates (r,ϕ,z) (r denotes the radial distance from the propagation axis, ϕ denotes the azimuthal angle, and z denotes the propagation distance) as follows [10]:

$$u_{m,p}(r,\phi,z) = \sqrt{\frac{2p!}{\pi(p+|m|)!}}\frac{1}{w(z)}\left[\frac{r\sqrt{2}}{w(z)}\right]^{|m|} L_p^m\left(\frac{2r^2}{w^2(z)}\right) e^{-\frac{r^2}{w^2(z)}} e^{-\frac{jkr^2 z}{2\left(z^2+z_R^2\right)}} e^{j(2p+|m|+1)\tan^{-1}\frac{z}{z_R}} e^{-jm\phi}, \tag{2}$$

where $L_p^m(\cdot)$ is the associated Laguerre polynomial with p and m representing the radial and angular mode numbers, respectively, and $w(z)$ is defined by $w(z) = w_0\sqrt{1+(z/z_R)^2}$, where w_0 is the zero-order Gaussian radius at the waist, $z_R = \pi w_0^2/\lambda$ is the Rayleigh range with λ being the wavelength, and $k = 2\pi/\lambda$ is the propagation constant. It can be seen from Eq. (2) that the mth mode of an LG beam has the azimuthal angular dependence of the form $\exp(-jm\phi)$, and consequently, m is also called the azimuthal mode number (index). For

#142928 - $15.00 USD Received 18 Feb 2011; revised 17 Mar 2011; accepted 18 Mar 2011; published 24 Mar 2011

$m=0$, $u(r,\phi,z)$ becomes a zero-order Gaussian beam, that is the TEM_{00} mode. For $p=0$, $L_p^m(\cdot)=1$ for all *m*s, and thus the intensity of an LG mode is a ring of radius proportional to $\sqrt{|m|}$.

It can be shown that for a fixed *p*, the following principle of orthogonality is satisfied:

$$\left(u_{m,p},u_{n,p}\right)=\int u_{m,p}^{*}\left(r,\phi,z\right)u_{n,p}\left(r,\phi,z\right)rdrd\phi=\begin{cases}\int\left|u_{m,p}\right|^{2}rdrd\phi, & n=m,\\ 0, & n\neq m.\end{cases} \tag{3}$$

because we have

$$\int_{-1}^{1}\frac{P_p^m\left(x\right)P_p^n\left(x\right)}{1-x^2}dx=\begin{cases}0, & m\neq n,\\ \dfrac{\left(p+m\right)!}{m\left(p-m\right)!}, & m=n\neq 0,\\ \infty, & m=n=0.\end{cases} \tag{4}$$

Therefore, different OAM "states" corresponding to a fixed *p* are all orthogonal with one another, and hence, they can be used as basis functions for *OAM modulation*.

Another important concept is spatial-domain multiplexing. Spatial-domain multiplexing in MMFs relies on skew rays or helical rays that spiral around the fiber's axis as they propagate along the fiber. Light following a helical path forms an optical vortex. The topological charge of the vortex depends on the number of complete turns around the axis in one wavelength. In other words, the integration of the phase around a closed path yields an integer multiple of 2π. Thus we can deduce that skew rays possess an orbital angular momentum. For an axially symmetric multimode fiber with a refractive index of $n^2\left(R\right)=n_1^2\left[1-2\Delta f\left(R\right)\right]$, where $f\left(R\right)$ is the refractive index profile as a function of radial distance *R*, the solution for the electric filed distribution takes the form [30]

$$\boldsymbol{e}=\hat{\boldsymbol{e}}^{\pm}\exp\left(\pm jm\phi\right)F_m\left(R\right)\exp\left(j\beta z\right), \tag{5}$$

where $\hat{\boldsymbol{e}}^{\pm}$ is the unit vector of the right (+)/left (-) circular polarization, ϕ is the azimuthal angle, *m* is the azimuthal index ($m=0,\ 1,\ 2,\ \ldots$), and β is the propagation constant. The term $\exp(\pm jm\phi)$ denotes the azimuthal phase dependence, and the radial function $F_m(R)$ can be found from the eigenvalue equation. The azimuthal dependence of Eq. (5) is the same as that of the LG modes, indicating that skew rays indeed possess an OAM.

In addition, both for multiplexing and modulation, in step-index fibers, the general solution of electric field along the z-axis is given by [32]

$$E_z=AJ_m\left(p\rho\right)\exp\left(jm\phi\right)\exp\left(j\beta z\right);\ \ \rho\leq a \tag{6}$$

where *a* is a core radius and $J_m(x)$ is the Bessel function of the first kind and order *m*. Similarly as in Eq. (5), the azimuthal dependence $\exp(jm\phi)$ indicates that Bessel modes given by Eq. (6) also possess OAM. Details on the generation of OAM modes with large angular momentum can be found in [33].

#142928 - $15.00 USD Received 18 Feb 2011; revised 17 Mar 2011; accepted 18 Mar 2011; published 24 Mar 2011

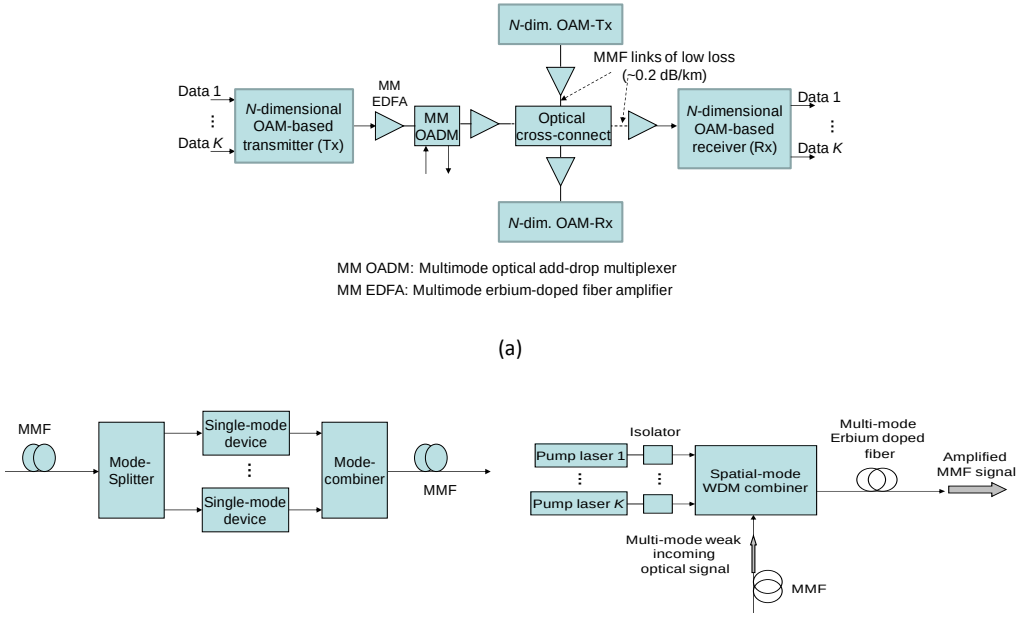

Fig. 1. (a) Conceptual diagram of a future MMF-supported network. (b) Block diagram of a multimode compatible passive optical device. (c) Block diagram of multimode compatible EDFA.

3. Spatial-mode-supported network and spatial-mode-compatible optical devices

The goal of our proposed approach is to increase the photon efficiency by increasing the number of degrees of freedom. Our reasoning stems from the Shannon's capacity formula. Shannon's theory establishes that the information capacity is given by

$$C(X,Y) = (N/2)\log\left(1+\sigma_x^2/\sigma_z^2\right) \text{bits per channel use,} \qquad (7)$$

where σ_x^2 is the variance of the source and σ_z^2 is the variance of the noise. Therefore, the information capacity is a logarithmic function of the signal-to-noise ratio (SNR) and a linear function of the number of dimensions *N*. The channel capacity formula indicates that the photon efficiency can be dramatically improved by increasing the number of dimensions, which we propose to achieve using OAM basis functions introduced in Section 2. The total aggregate data rate can also be significantly increased as long as the orthogonality among OAM basis functions is preserved. Some initial results for free-space optical channel have been provided by the authors recently [8]; however, the use of OAM modes in MMF links as multidimensional basis functions is a new research topic, which is addressed here for the first time.

MMFs are traditionally considered as mediums for short-reach applications. However, the recent experiment [11], in which 21.4 Gb/s polarization-multiplexed coherent OFDM transmission over 200 km of MMF has been demonstrated, indicates that MMFs can be used for metro and medium-haul applications, as well. Today's MMFs are however far away from being a medium suitable for long-haul transmission. The main issues are related to high loss and to the use of an excessive number of modes that overwhelms the computational capabilities of currently existing silicon chips. Novel types of MMFs with small number of

#142928 - $15.00 USD Received 18 Feb 2011; revised 17 Mar 2011; accepted 18 Mar 2011; published 24 Mar 2011

orthogonal modes (possibly several) and with low attenuation coefficients are needed. A promising methodology is to extend the well-developed theory behind dual-mode optical fibers [24–27]. To elaborate, it was found in [26] that the group delay difference between LP_{01} and LP_{11} modes vanishes at the normalized frequency of $V_0 = 6.8,$ which is just below the cutoff frequency of the third mode. The corresponding core diameter and the refractive index difference at $\lambda = 1380$ nm are 24.8 μm and $\Delta = \left(n_1^2 - n_2^2\right) / 2n_1^2 = 0.3\%,$ where n_1 (n_2) is the refractive index of the core (cladding), respectively. The optimum index profile of dual-mode fibers with zero intermodal dispersion at $\lambda = 1550$ nm is derived by Cvijetic [26,27]. By using a similar methodology, it is possible to develop the optimum index profile that can support *N* spatial modes with low dispersion.

The conceptual diagram of an MMF-based optical network is shown in Fig. 1(a). We can identify several critical devices to be developed in the foreseeable future. The most important MMF network devices are: MMF multiplexers/demultiplexers, MMF amplifiers, and MMF optical add-drop multiplexers. The current passive devices in optical fiber networks are single-mode based and are highly wavelength dependent, and will not work as desired when a multimode signal is present. A possible solution for a spatial-mode scenario is illustrated in Fig. 1(b). The spatial-mode signal is first split using a mode-demultiplexer, and then each mode is processed by the corresponding SMF component, and finally, the resulting SMF signals are combined using a mode-multiplexer. The optical amplifier is probably the most critical component here, and it can be implemented as illustrated in Fig. 1(c). The weak spatial-mode signal and the corresponding pump signals are combined together by using a combiner implementing spatial-mode wavelength division multiplexing (WDM). To avoid the mode-dependent gain problem, the pumps should be independently adjusted so that different spatial-modes have the same output power level.

The operating principle for spatial-domain-based modulation is illustrated in Fig. 2(a). The *N*-dimensional OAM-based transmitter depicted in Fig. 1(a) is built upon this principle. First, a continuous wave laser diode signal is split into *N* branches by using a power splitter (1:*N* star coupler) to feed *N* electro-optic modulators (EO MODs), such as Mach-Zehnder modulators (MZMs) or I/Q-modulators (I/Q-MODs), each corresponding to one of the *N* OAM modes. As shown in Fig. 2(a), the other input to the *i*th EO MOD, $1 \le i \le N,$ is the *i*th coordinate of the signal to be modulated. For example, if an *N*-dimensional signal constellation is used, each EO MOD receives a real-valued number at its input. Thus, an MZM suffices for modulation. On the other hand, one can employ a 2*N*-dimensional signal constellation and feed the resulting 2*N* coordinate values as *N* complex numbers, each containing two coordinates, into the EO MODs. In this case, I/Q-MODs can be used for modulation, and hence, we can refer to each I/Q-MOD as a 2D modulator. We depict in Fig. 2(b) the infrastructure of an EO MOD featuring an I/Q-MOD.

#142928 - $15.00 USD Received 18 Feb 2011; revised 17 Mar 2011; accepted 18 Mar 2011; published 24 Mar 2011

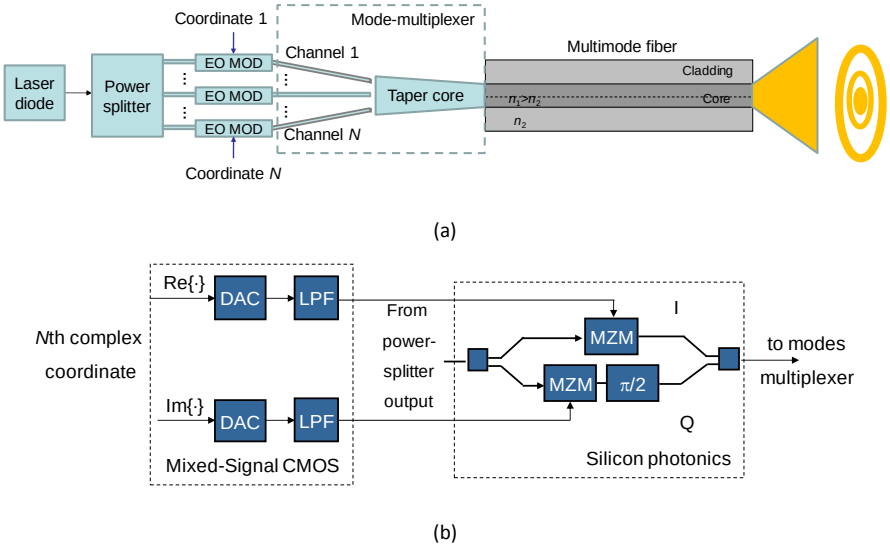

Fig. 2. (a) Illustration of spatial-domain-based *N*-dimensional modulation. An electro-optical modulator (EO MOD) can be a 1D (MZM), a 2D (I/Q-modulator), or a 4D modulator (see [7]). (b) Details of an optical 2D modulator, i.e., I/Q-modulator. EO MOD: electro-optical modulator. MZM: Mach-Zehnder Modulator. DAC: Digital-to-analog converter. LPF: Low-pass filter.

As a final option for EO MODs, we should add 4D modulators, which were discussed in detail in our previous papers [5,7]. In this case, in addition to *N* OAM modes and two quadratures (I and Q), we propose using two orthogonal SAM modes so that the signal constellation can be defined over a 4*N*-dimensional signal space. We refer interested readers to [5,7] for implementation details on a 4D modulator. The scenarios discussed above for spatial-domain-based modulation concerns long-haul applications. For medium-haul and short-haul applications, the *N*-dimensional direct detection version should result in satisfactory performance. Following the EO MODs is the mode-multiplexer. As depicted in Fig. 2(a), *N* independent electrical data streams at the outputs of *N* EO MODs are fed into the mode-multiplexer, which is implemented by using *N* waveguides and taper-core fiber. The tapper core fiber should be properly designed so that orthogonal OAM modes are excited in MMF. At the end of the MMF link, the corresponding signal is mode-demultiplexed. The mode-demultiplexer can be implemented in a similar fashion to the mode-multiplexer. Such an implementation requires the use of the orthogonal demultiplexed modes as inputs to the corresponding set of *N* photodetectors. Instead of using *N* different photodetectors for different modes, it is possible to fabricate a donut-shaped photodetector [13–18], which is able to simultaneously detect all separate OAM modes of interest.

#142928 - $15.00 USD Received 18 Feb 2011; revised 17 Mar 2011; accepted 18 Mar 2011; published 24 Mar 2011

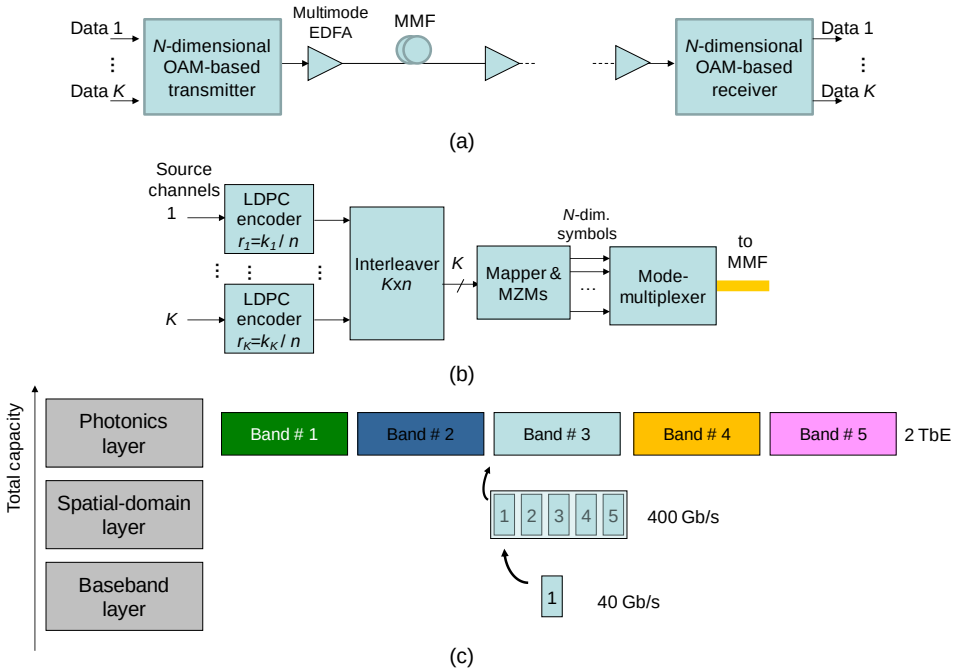

Fig. 3. (a) System configuration and (b) transmitter configuration for the proposed multidimensional LDPC-coded OAM-based modulation scheme for transmission over MMFs. (c) Conceptual diagram for achieving 4 TbE using the proposed scheme with five OAM modes to define a five-dimensional modulation and four amplitudes per dimension, i.e. 2 channel bits per OAM mode (see Eq. (9)). (In (c), only one polarization branch is shown.)

There are many open problems that remain to be solved before mode-multiplexed and polarization-multiplexed, coded, multiband optical system enabling multi-Tb/s optical transport becomes a reality. These pertain to: (i) the fabrication of MMFs with low attenuation and optimum profile index, enabling zero multimode dispersion, (ii) the development of both passive and active MMF devices discussed above, (iii) the analysis of the nonlinear interaction among different modes from both polarizations, and (iv) the development of efficient modulation and coding schemes enabling multi-Tb/s optical transport over MMFs. In the next section, we describe our proposed coded-modulation scheme for an MMF-supported multi-Tb/s optical transport.

4. Spatial-domain-based multidimensional LDPC-coded modulation

We introduced spatial-domain modulation principles in Section 3. In this section, we provide a detailed treatment on our proposed spatial-domain-based multidimensional LDPC-coded modulation approach to enable multi-Tb/s optical transport. The proposed approach employs N OAM modes for modulation; however, the signal space can be N-, or $2N$-, or even $4N$-dimensional, as mentioned in the previous section. Here, without loss of generality, we describe the N-dimensional modulation case, and hence the corresponding signal constellation coordinates are real-number-valued and the EO MODs in Fig. 2(a) are simply MZMs.

By increasing the number of dimensions, i.e., the number of orthogonal OAM basis functions, N, we can increase the aggregate data rate of the system while ensuring reliable transmission at these ultra-high speeds using capacity-approaching low-density parity-check (LDPC) codes [31] at each level. Apart from increasing the aggregate data rate, an N-dimensional $(N>2)$ space when compared to the conventional two-dimensional (2D) space can provide larger Euclidean distances between signal constellation points, resulting in better BER performance. The overall system configuration and the transmitter configuration are depicted in Fig. 3. As shown in Fig. 3(b), K independent bit streams coming from different

#142928 - $15.00 USD Received 18 Feb 2011; revised 17 Mar 2011; accepted 18 Mar 2011; published 24 Mar 2011

information sources are first encoded using binary LDPC codes, which do not have to be identical codes. The outputs of the encoders are then interleaved by a $(K \times n)$ block interleaver. The block interleaver accepts data from the encoders row-wise, and outputs the data column-wise to the mapper that accepts *K* bits at the time instance *i*. The mapper determines the corresponding *Q*-ary signal constellation point, where $Q = M^N$ and *M* is the number of amplitude levels per dimension, using

$$s_i = C_N \sum_{j=1}^{N} \varphi_{i,j} \Phi_j, \tag{8}$$

where the set $\{\Phi_1, \Phi_2, \ldots, \Phi_N\}$ represents the set of *N* orthonormal OAM basis functions, and C_N stands for a normalization factor. Each coordinate of the *N*-dimensional mapper output is passed as the RF input to one of the *N* MZMs integrated on the same chip. Finally, the modulated signals are sent over the MMF system of interest after being combined into an optical wave via a mode-multiplexer, which was discussed in Fig. 2(a).

The number of bits per signal constellation point is determined by $\log_2 Q = \log_2(M^N) = K$. The dimensionality, *N*, and number of amplitude levels per dimension, *M*, can be adjusted according to the desired final rate. To achieve an aggregate information bit rate of 4 Tb/s, for example, we can use the proposed scheme with polarization multiplexing and carry on each polarization 2 Tb/s information stream. The conceptual diagram for 4 TbE based on the proposed scheme is presented in Fig. 3(c). As shown in the figure, the baseband can originate from a 40 GbE line. However, 10 Gb/s baseband can also be used, and in this case, we have to perform 4:1 RF multiplexing. This RF layer is optional and hence it is not shown in Fig. 3(c). Having 40 Gb/s baseband traffic, we can set $M = 4$ and $N = 5$ to achieve an aggregate information bit rate of 400 Gb/s after mode-multiplexing, i.e. at the spatial-domain layer. The third layer in Fig. 3(c), which we refer to as the photonic layer, is implemented by combining the signals from five frequency locked lasers into a 2 Tb/s serial optical transport signal. Finally, polarization-multiplexing is achieved to couple the 4 Tb/s optical signal into the fiber. In general terms, the proposed scheme using *N* OAM modes and *M* amplitude levels in each one of the *N* dimensions of the signal constellation attains an aggregate bit rate of

$$\begin{aligned} 2 \times \log_2(M^N) \ \frac{\text{ch. bits}}{\text{ch. sym.}} \times R_s \ \frac{\text{ch. sym.}}{\text{s}} \times r \ \frac{\text{info. bits}}{\text{ch. bits}} = \\ 2 \times N \ \frac{\text{modes}}{\text{info. sym.}} \times \log_2(M) \ \frac{\text{info. bits}}{\text{mode}} \times R_i \ \frac{\text{info. sym}}{\text{s}}, \end{aligned} \tag{9}$$

where the factor of 2 stems from polarization-multiplexing, and where *r* is the code rate, which is assumed to be equal for LDPC codes at each level, R_s is the symbol rate, and R_i is the information symbol rate. As far as the implementation is concerned, the RF layer, which is used to perform RF multiplexing, can quite readily be implemented in mixed-circuit CMOS ASICs. The implementation of the spatial-domain layer comprised of modulators and mode-multiplexer was already discussed in Section 3 above. The photonics layer, on the other hand, can be implemented using photonic integrated circuit (PIC) technology, either in InP [28] or in Si [34]. Namely, all photonic building blocks can be implemented in silicon photonics, except for lasers that must be flip-chip bonded on top of the silicon die, and germanium photodetectors that should be placed on top of the silicon waveguides.

The receiver configurations for direct detection and coherent detection are depicted as in Figs. 4(a) and 4(b), respectively. To help ease in the comprehension of ideas, the simplest spatial-domain-based coded modulation scheme with direct detection can be described by the following set of constellation points for $N = 3$ and $M = 2$: {(0,0,0), (0,0,1), (0,1,0), (0,1,1),

#142928 - $15.00 USD Received 18 Feb 2011; revised 17 Mar 2011; accepted 18 Mar 2011; published 24 Mar 2011

(1,0,0), (1,0,1), (1,1,0), (1,1,1)}, while the corresponding coherent detection counterpart is obtained substituting 0s with −1s. (The normalization factor C_3 in Eq. (8) is omitted to simplify presentation.) The corresponding OAM modes can be selected from the set of azimuthal modes as follows {-1,0,1}. The signal constellation for coherent detection with $N=3$ and $M=4$ is given by: {(−3,-3,-3), (−3,-3,-1), (−3,-3,1), (−3,-3,3), …, (3,3,-3), (3,3,-1), (3,3,1), (3,3,3)}, with signal constellation points' coordinates being the amplitude levels. These modulation formats can be straightforwardly extended to higher dimensions. Returning back to the receiver configurations depicted in Fig. 4, we observe that the outputs of the N branches of the mode-detector, implemented as already discussed in Section 3 above, are sampled at the symbol rate and the corresponding samples are forwarded to an *a posteriori* probability (APP) demapper.

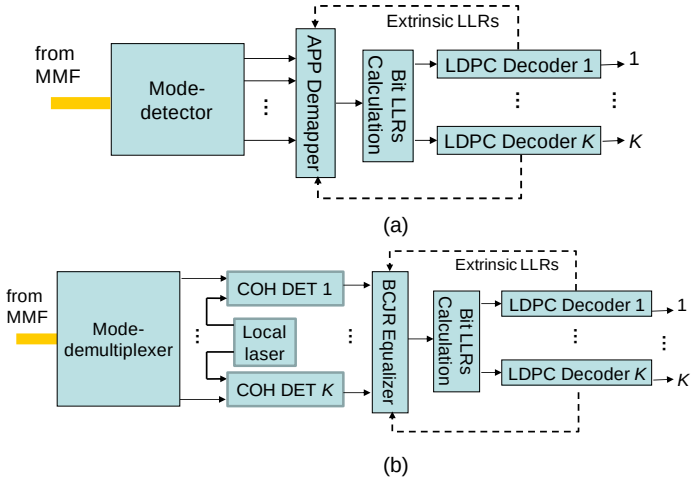

Fig. 4. (a) LDPC-coding based receiver configuration with direct detection, (d) LDPC coding based receiver configuration with coherent detection, where COH DET stands for a balanced coherent detector.

The demapper provides the symbol log-likelihood ratios (LLRs), which are used by the bit LLR calculation block to compute bit LLRs required for iterative decoding in binary LDPC decoders. To improve the overall system performance, we iterate extrinsic information between LDPC decoders and APP demapper until convergence or until a predetermined number of iterations has been reached. Finally, the outputs of the K binary LDPC decoders are provided to the user as the estimates of the K information streams sent by the transmitter.

From the description of the transmitter and the receiver setups, it is clear that the system is scalable to any number of dimensions with small penalty in terms of BER performance, as long as the orthonormality between OAM states is preserved. The orthogonality among OAM modes in realistic multimode or multicore fibers can be re-established by various MIMO and equalization techniques. It is important to notice that increasing the number of dimensions leads to an increased complexity, and hence, a compromise between the desired aggregate rate and the complexity of the system should be made in practice.

5. Performance analysis

We evaluate the BER performance of the proposed spatial-domain-based multidimensional LDPC-coded modulation and compare it against the performance of the corresponding coded polarization-multiplexed quadrature amplitude modulation (QAM) scheme and to that of the corresponding 4D coded modulation scheme that we proposed in [7]. We performed Monte Carlo simulations for the amplified spontaneous emission (ASE) noise scenario for 3 APP demapper-LDPC decoder iterations and 25 LDPC decoder inner iterations. Results of simulations are presented in Fig. 5 for the symbol rate of 31.25 GS/s. We should note that the

#142928 - $15.00 USD Received 18 Feb 2011; revised 17 Mar 2011; accepted 18 Mar 2011; published 24 Mar 2011

symbol rate used here, which is 31.25 GS/s, is smaller than that used used in [7], which was 50 GS/s. That is, because of the additional degrees of freedom offered by the proposed spatial-domain-based coded multidimensional modulation, we can relax the requirement on symbol rate while still achieving multi-Tb/s aggregate information bit rates per single wavelength. This is an important advantage offered by the proposed scheme. By setting $M=2$ and $N=8$, and using component LDPC codes of code rate of $r=0.8$, the aggregate information bit rate (see Eq. (9)) attained by the proposed scheme reaches $2\times 8\times 1\times 31.25\times 0.8=400$ Gb/s, which is compatible with the next generation 400 GbE. If instead, we set $M=2$ and $N=16$ while keeping all other parameters intact, the aggregate information bit rate becomes 800 Gb/s. For fair comparison among various multilevel and multidimensional modulation schemes we use OSNR per information bit. The OSNR per information bit is defined as $OSNR_S/\log_2(M^N)$, where $OSNR_S$ is symbol OSNR per single polarization.

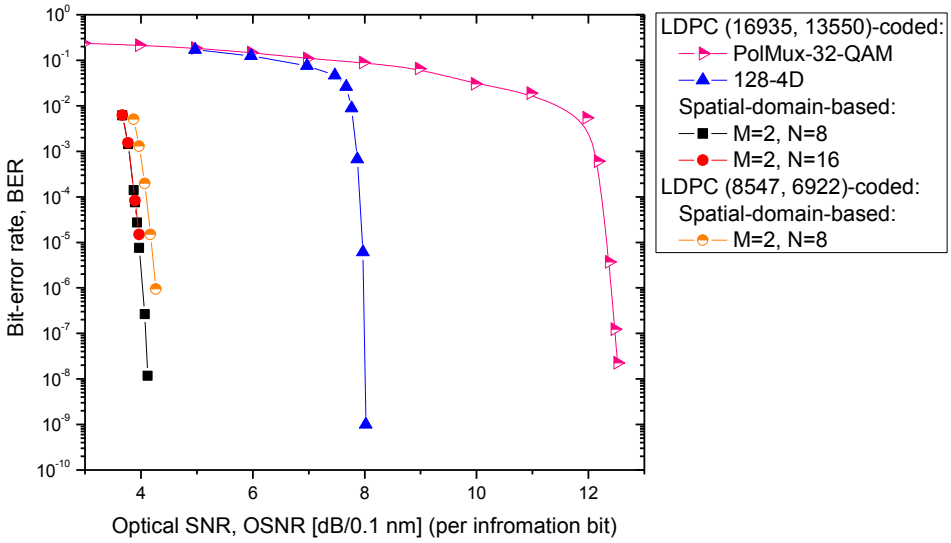

Fig. 5. BER performance of spatial-mode-based LDPC-coded multidimensional modulation schemes per single band and per single polarization.

From Fig. 5, we observe that spatial-domain-based LDPC(16935,13550)-coded 8D modulation outperforms a 128-point 4D modulation by 3.88 dB at BER of 10^{-8} while achieving 120 Gb/s higher aggregate information bit rate as the latter scheme achieves only $7\times 50\times 0.8=280$ Gb/s of aggregate information bit rate. Compared to the corresponding polarization-multiplexed 32-QAM scheme, which achieves the same aggregate information bit rate ($2\times 5\times 50\times 0.8=400$ Gb/s), the proposed scheme provides a striking additional coding gain of 8.39 dB at the BER of 10^{-8}. As we stated above, doubling the number of dimensions from 8 to 16 doubles the aggregate information bit rate, and as we can conclude from Fig. 5, it results no distinguishable degradation in BER performance if orthogonality between dimensions is preserved. Our final comparison pertains to the effect of the component LDPC codes chosen for error correction. Until now, we discussed schemes which employ at each level LDPC(16935,13550) code, which is a rate-0.8 code of column weight 3. If, instead, we use LDPC(8547,6922) code of the same rate but of column weight 4 and of length 8547, which is nearly half the length of LDPC (16935,13550) code, then we observe from Fig. 5 that we lose about 0.15 dB for the BER of 10^{-8}.

#142928 - $15.00 USD Received 18 Feb 2011; revised 17 Mar 2011; accepted 18 Mar 2011; published 24 Mar 2011

6. Concluding remarks and future work

Inspired by high potential of multidimensional signal constellations [5–8] and recent demonstrations [13–21] in which OAM modes are successfully excited in MMFs, we proposed the use of spatial-domain-based coded multidimensional modulation as an enabling technology for multi-Tb/s serial optical transport. We demonstrated by simulations that 8D spatial-domain-based coded modulation scheme outperforms a 4D coded-modulation scheme by 3.88 dB at the BER of 10^{-8} while providing 120 Gb/s higher aggregate information bit rate. We also showed that the proposed scheme outperforms the corresponding conventional polarization-multiplexed coded-QAM scheme by even a larger, and indeed striking, margin of 8.39 dB at the BER of 10^{-8}.

We also described the MMF based optical network, identified its key optical components, such as mode–multiplexer and mode-demultiplexer, MMF amplifier, MMF optical add-drop multiplexer, and mode-detector. Furthermore, we discussed how they can be implemented. We also described how the proposed scheme can be used for multi-Tb/s serial optical transport by using the example 4 TbE based on the proposed scheme.

For the future work, interesting research problems would include: (i) integration of the power combiner, a series of EO MODs and the mode-multiplexer shown in Fig. 2(a) into a single chip; and (ii) for *N*-dimensional direct detection scheme, integration of mode-demultiplexer and a series of photodetectors or alternatively the donut-based photodetector into a single chip.

Acknowledgments

This work was supported in part by the National Science Foundation (NSF) under Grants CCF-0952711 and ECCS-0725405; through NSF CIAN ERC Center for Integrated Access Network under grant EEC-0812072; and in part by NEC Labs.

#142928 - $15.00 USD Received 18 Feb 2011; revised 17 Mar 2011; accepted 18 Mar 2011; published 24 Mar 2011